

## MYELOID NEOPLASIA

## Ceramide-induced integrated stress response overcomes Bcl-2 inhibitor resistance in acute myeloid leukemia

Alexander C. Lewis,<sup>1</sup> Victoria S. Pope,<sup>1</sup> Melinda N. Tea,<sup>1</sup> Manjun Li,<sup>1</sup> Gus O. Nwosu,<sup>1</sup> Thao M. Nguyen,<sup>1,2</sup> Craig T. Wallington-Beddoe,<sup>1-4</sup> Paul A. B. Moretti,<sup>1</sup> Dovile Anderson,<sup>5</sup> Darren J. Creek,<sup>5</sup> Maurizio Costabile,<sup>1,6</sup> Saira R. Ali,<sup>1</sup> Chloe A. L. Thompson-Peach,<sup>2,7</sup> B. Kate Dredge,<sup>1</sup> Andrew G. Bert,<sup>1</sup> Gregory J. Goodall,<sup>1</sup> Paul G. Ekert,<sup>8-10</sup> Anna L. Brown,<sup>1,2,11</sup> Richard D'Andrea,<sup>1</sup> Nirmal Robinson,<sup>1</sup> Melissa R. Pitman,<sup>1,12</sup> Daniel Thomas,<sup>2,7,13</sup> David M. Ross,<sup>1-4,7,14</sup> Briony L. Gliddon,<sup>1</sup> Jason A. Powell,<sup>1,2,\*</sup> and Stuart M. Pitson<sup>1,2,12,\*</sup>

<sup>1</sup>Centre for Cancer Biology, University of South Australia and SA Pathology, Adelaide, SA, Australia; <sup>2</sup>Faculty of Health Sciences, Adelaide Medical School, University of Adelaide, Adelaide, SA, Australia; <sup>3</sup>College of Medicine and Public Health, Flinders University, Bedford Park, SA, Australia; <sup>4</sup>Flinders Medical Centre, Bedford Park, SA, Australia; <sup>5</sup>Drug Delivery, Disposition, and Dynamics, Monash Institute of Pharmaceutical Sciences, Monash University, Parkville, VIC, Australia; <sup>6</sup>Clinical and Health Sciences, University of South Australia, Adelaide, SA, Australia; <sup>7</sup>Precision Medicine Theme, South Australian Health and Medical Research Institute, Adelaide, SA, Australia; <sup>8</sup>Children's Cancer Institute, Lowy Cancer Research Centre, University of New South Wales, Sydney, NSW, Australia; <sup>9</sup>Peter MacCallum Cancer Centre, Melbourne, VIC, Australia; <sup>10</sup>Murdoch Children's Research Institute, Royal Children's Hospital, Parkville, VIC, Australia; <sup>11</sup>Department of Genetics and Molecular Pathology, SA Pathology, Adelaide, SA, Australia; <sup>12</sup>School of Biological Sciences, University of Adelaide, Adelaide, SA, Australia; <sup>13</sup>Institute for Stem Cell Biology and Regenerative Medicine, Stanford School of Medicine, Stanford University, Stanford, CA; and <sup>14</sup>Department of Haematology and Bone Marrow Transplantation, Royal Adelaide Hospital, Adelaide, SA, Australia

## KEY POINTS

- Enhancing cellular ceramide levels in AML activates protein kinase R to induce the integrated stress response.
- The ISR induces the BH3-only protein Noxa, causing degradation of Mcl-1 and sensitization of AML to Bcl-2 inhibition.

**Inducing cell death by the sphingolipid ceramide is a potential anticancer strategy, but the underlying mechanisms remain poorly defined. In this study, triggering an accumulation of ceramide in acute myeloid leukemia (AML) cells by inhibition of sphingosine kinase induced an apoptotic integrated stress response (ISR) through protein kinase R-mediated activation of the master transcription factor ATF4. This effect led to transcription of the BH3-only protein Noxa and degradation of the prosurvival Mcl-1 protein on which AML cells are highly dependent for survival. Targeting this novel ISR pathway, in combination with the Bcl-2 inhibitor venetoclax, synergistically killed primary AML blasts, including those with venetoclax-resistant mutations, as well as immunophenotypic leukemic stem cells, and reduced leukemic engraftment in patient-derived AML xenografts. Collectively, these findings provide mechanistic insight into the anticancer effects of ceramide and preclinical evidence for new approaches to augment Bcl-2 inhibition in the therapy of AML and other cancers with high Mcl-1 dependency.**

## Introduction

The discovery of novel signaling mechanisms that enable induction of proapoptotic BH3-only proteins independent of TP53 has immense therapeutic potential for both TP53 mutant cancer and tumors resistant to Bcl-2 inhibitors. Proapoptotic Noxa is a Bcl-2 family protein that belongs to a subclass of BH3-only proteins and can induce apoptosis via both TP53-dependent and -independent processes, depending on the cellular context. Certain cytotoxic drugs have been shown to upregulate Noxa protein, principally through upregulating messenger RNA transcription,<sup>1</sup> but the upstream signals and physiological stimuli are not well defined, nor are they optimized for therapy. Through its ability to bind and neutralize both A1 and Mcl-1 prosurvival proteins, upregulation of Noxa<sup>2</sup> has therapeutic potential in multiple cancers that show intrinsic or acquired resistance to Bcl-2 inhibitor therapies, such as venetoclax.

The BH3 mimetic, venetoclax is a highly selective oral inhibitor of the prosurvival protein Bcl-2 approved for treatment of 17p(del) chronic lymphocytic leukemia.<sup>3</sup> Venetoclax shows modest activity as a single agent in acute myeloid leukemia (AML; overall response rate, 19%)<sup>4</sup> but promising results when combined with chemotherapy (complete response, 62%) or hypomethylating agents (complete response, 67%),<sup>5,6</sup> and has been recently approved by the FDA in adults who are  $\geq 75$  years of age or who have comorbidities precluding intensive induction chemotherapy (registered on clinicaltrials.gov as NCT02993523 and NCT03069352). Unlike lymphoid leukemias, AML cells rely on the prosurvival protein Mcl-1 for disease maintenance,<sup>7</sup> suggesting that its inhibition may prove beneficial in achieving deep molecular remission. Preclinical studies revealed Mcl-1 as a biomarker for venetoclax resistance caused by the inability of the drug to sequester Mcl-1, highlighting the importance of concurrent inhibition of multiple proteins in the Bcl-2 family.<sup>4,8</sup>

An alternative mechanism for induction of programmed cell death can occur through the ceramide/sphingosine-1-phosphate (S1P) rheostat.<sup>9</sup> Ceramide accumulation is thought to contribute to the effects of many anticancer therapies, including ionizing radiation, daunorubicin, etoposide, and gemcitabine, as well as some targeted therapies, such as tyrosine kinase inhibitors.<sup>10</sup> Ceramides are lipids present in high concentrations in cell membranes, but they accumulate after blockade of downstream conversion of sphingosine to S1P, which occurs principally through the activity of sphingosine kinase 1 (SPHK1). SPHK1 can promote tumorigenic pathways, such as survival and proliferation in multiple solid and blood cancers, and is a key player of the sphingolipid rheostat in maintaining the balance between proapoptotic ceramide and sphingosine and prosurvival,<sup>11</sup> but, how sphingolipid signaling integrates with intrinsic BAX/BAK-dependent apoptosis is not well understood.

We have demonstrated that targeting SPHK1 in AML depletes the prosurvival protein Mcl-1 and can synergize with the Bcl-2/Bcl-X<sub>L</sub> inhibitor navitoclax.<sup>12</sup> However, the mechanistic basis of synergy between SPHK1 inhibition and navitoclax remained poorly defined. In this study, triggering accumulation of ceramide in AML cells by inhibition of SPHK1 induced upregulation of the BH3-only protein Noxa via ceramide-mediated activation of protein kinase R (PKR), as part of the integrated stress response (ISR) pathway, and subsequent activation of the transcription factor ATF4. Targeting this novel pathway induced synergy with the clinically relevant Bcl-2 inhibitor venetoclax to exert antileukemic activity against blasts from AML patients, including those harboring mutations associated with venetoclax resistance and immunophenotypic CD34<sup>+</sup>CD38<sup>-</sup>CD123<sup>+</sup> leukemic stem cells (LSCs), both in vitro and in vivo. This finding advocates for the use of ceramide-modulating agents as ISR activators to augment Bcl-2 inhibiting strategies for the treatment of AML and other cancers with high dependency on Mcl-1.

## Methods

Additional details are provided in supplemental Methods (available on the *Blood* Web site).

### Study approval

Animal studies were approved by the SA Pathology/CALHN (Central Adelaide Local Health Network) and UniSA (University of South Adelaide) animal ethics committees. Human samples were obtained from the South Australian Cancer Research Biobank from patients with AML after informed consent was received, and the experiments were approved by the Royal Adelaide Hospital Human Ethics Committee (Protocol 041009).

### Mutational analysis of primary AML biopsies

Mutations in primary AML biopsies were identified by either whole-exome sequencing or targeted gene sequencing, as described previously.<sup>12</sup>

### Cell lines and primary AML samples

The AML cell lines MV411, THP-1, MOLM13, and UT7 were cultured as previously described.<sup>12</sup> OCI-AML3 cells were cultured in RPMI with 10% fetal calf serum (FCS; HyClone Thermo Scientific), HL-60 cells in Iscove's modified Dulbecco's medium

(IMDM) with 20% FCS, and HEK293T cells in Dulbecco's modified Eagle's medium (DMEM) with 10% FCS. Cell line authentication was confirmed by short tandem repeat profiling. Mononuclear cells from diagnostic bone marrow or apheresis product samples were isolated by Ficoll-Hypaque density-gradient centrifugation and resuspended in IMDM containing 10% FCS. Factor-dependent myeloid wild-type and Bax<sup>-/-</sup>/Bak<sup>-/-</sup> cells were cultured in DMEM (low glucose) supplemented with 10% FCS and 0.25 ng/mL murine interleukin-3. Parental and PERK<sup>-/-</sup> HAP1 cells (Horizon Discovery) were cultured in IMDM containing 10% FCS.

### In vivo primary AML xenograft model

Six-week-old female NOD/SCID/IL-2Rγ<sup>-/-</sup> (NSG) mice were injected IV with 5 × 10<sup>6</sup> human primary AML cells. The mice were tail bled weekly to confirm human cell engraftment by flow cytometry (>1% hCD45<sup>+</sup>). MP-A08 (100 mg/kg intraperitoneally [PEG 400]) and venetoclax (75 mg/kg orally [60% Phosal 50PG, 30% PEG 400, and 10% ethanol]) were administered daily for 2 weeks. Mice were euthanized after cessation of treatment, and bone marrow was collected to measure hCD45<sup>+</sup> cells by flow cytometry. Immunohistochemistry on the mouse sternum was performed as previously described, by using the human-specific mitochondrial antibody (Thermo Fisher Scientific cat. no. MA1-21891).<sup>12</sup>

## Results

### BH3-only protein Noxa is essential for AML cell death induced by SPHK1 inhibition

Previous studies have shown that SPHK1 inhibitors, including MP-A08, induce AML cell death.<sup>12-16</sup> We have also shown that this occurs in an Mcl-1-dependent manner<sup>12</sup>; however, the exact mechanism has remained unclear. The BH3-only protein Noxa is a selective binding partner of Mcl-1, and this interaction is known to promote Mcl-1 degradation and induction of apoptosis.<sup>17</sup> Treatment of MV411 AML cells with the SPHK1 inhibitor MP-A08 increased Noxa expression and augmented the association of Noxa with Mcl-1 (Figure 1A). The increase in Noxa protein expression coincided with increased Noxa messenger RNA levels after MP-A08 treatment (Figure 1B; supplemental Figure 1) and was blocked through inhibition of protein synthesis by cycloheximide (Figure 1C), suggesting that increased Noxa expression occurs via transcriptional upregulation. Similar increases in Noxa expression were observed in both MV411 cells and primary samples from patients with AML (supplemental Table 1) in response to another structurally different SPHK1 inhibitor, SK1-I (supplemental Figure 2). A broader analysis of Bcl-2 and BH3-only proteins in response to MP-A08 before apoptosis induction (6 hours) in multiple AML cell lines revealed dose-dependent increases in Noxa and, to a lesser extent, other BH3-only proteins Bim and cleaved Bid, but not other Bcl-2 family proteins or TP53 (Figure 1D-E; supplemental Figure 3A-B). Doxycycline-inducible short hairpin RNA (shRNA) knockdown of Noxa partially reversed the degradation of Mcl-1 and rescued the effects of MP-A08 on cell viability (Figure 1F; supplemental Figure 3C). In contrast, Bim knockdown had only a minor effect on cell viability (Figure 1G), but could not reverse loss of Mcl-1, whereas Bid knockdown had no effect (Figure 1H). This finding implicates Noxa as an important determinant of the apoptotic effects of SPHK1 inhibition in AML cells.

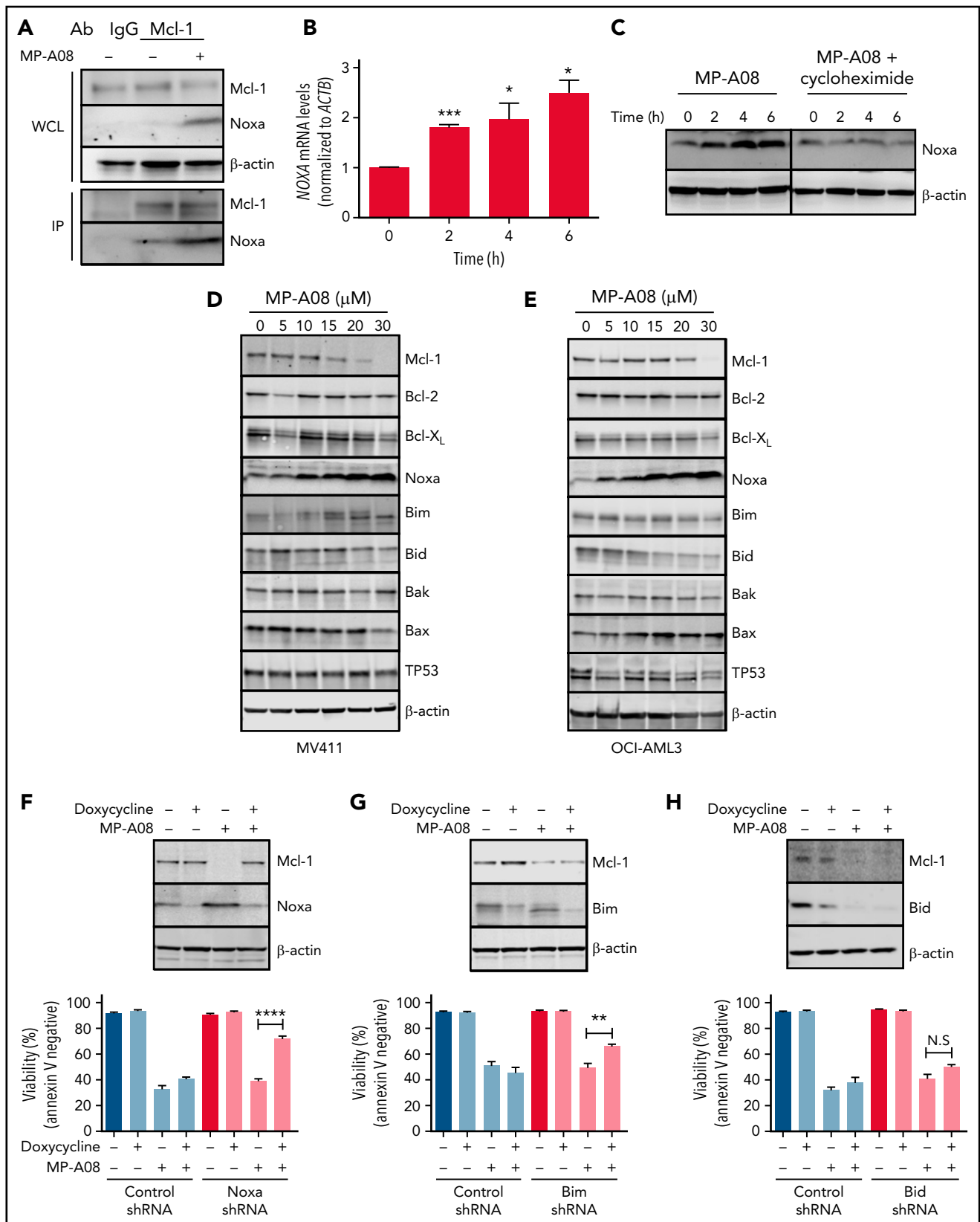


**Figure 1. The BH3-only proteins Noxa and Bim are essential for MP-A08-induced cell death.** (A) Mcl-1 immunoprecipitation of MV411 cells treated with MP-A08 for 6 hours and subjected to immunoblot analysis with the indicated antibodies. (B) Quantitative polymerase chain reaction analysis of MV411 cells treated with MP-A08 (20 μM) over 6 hours. (C) Immunoblot analysis of MV411 cells treated with MP-A08 in the presence of cycloheximide for 6 hours. MV411 (D) or OCI-AML3 (E) were treated with increasing concentrations of MP-A08 for 6 hours and subjected to immunoblot analysis with the indicated antibodies. MV411 cells were lentivirally transduced with shRNAs targeting Noxa (F), Bim (G), or Bid (H) and treated with doxycycline for 48 hours and MP-A08 (15 μM) for either 6 hours for immunoblot analysis or 24 hours for cell viability using Annexin V staining. All qualitative data are representative of at least 3 independent experiments, and all quantitative data are the mean ± standard error of the mean from 3 independent experiments. Statistical significance was assessed by Student t test. \**P* < .05; \*\**P* < .005; \*\*\**P* < .0001. N.S., not significant.

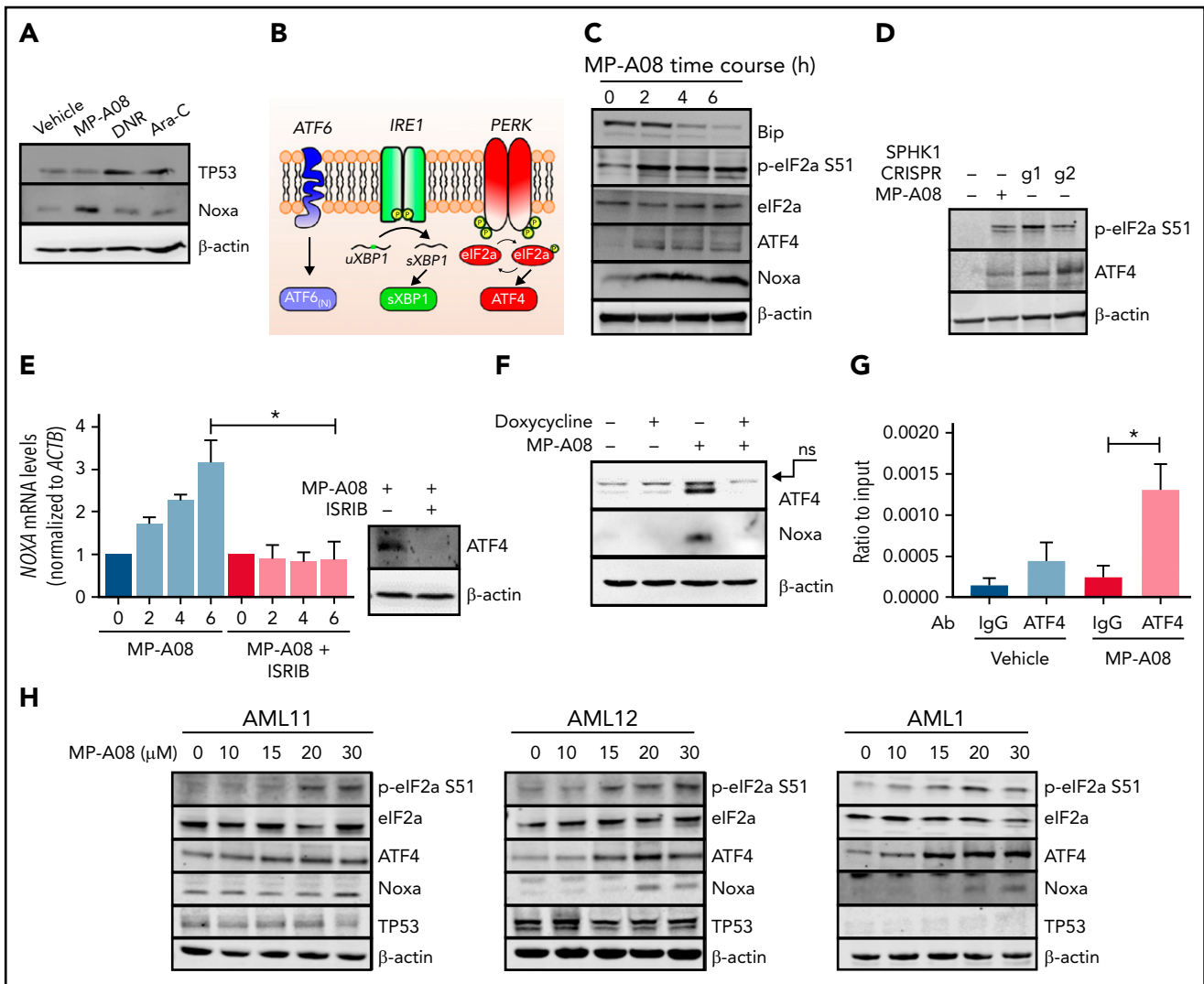


**Figure 2. MP-A08 induces ATF4 dependent Noxa transcription.** (A) MV411 cells were treated with MP-A08 (20  $\mu$ M), daunorubicin (DNR) (1  $\mu$ M), or cytarabine (Ara-C; 1  $\mu$ M) for 6 hours; lysed; and subjected to immunoblot analysis with the indicated antibodies. (B) The UPR. (C) MV411 cells were treated with MP-A08 (20  $\mu$ M) over a 6-hour period, lysed, and subjected to immunoblot analysis with the indicated antibodies. (D) MV411 cells were stably transduced with 2 different CRISPR guide sequences targeting SPHK1 (g1 and g2), lysed, and subjected to immunoblot analysis with the indicated antibodies. The efficiency of the SPHK1 knockout was confirmed via SPHK1 activity assays of lysates from those cells in assay conditions largely selective for SPHK1 over SPHK2 (supplemental Figure 5C). (E) MV411 cells were treated with MP-A08 (20  $\mu$ M), alone or in combination with the eIF2b agonist, ISRIB (200 nM) over 6 hours for quantitative polymerase chain reaction analysis of Noxa messenger RNA levels and immunoblot analysis with the indicated antibodies. Statistical significance was assessed by Student *t* test. \**P* < .05 (*n* = 3). (F) MV411 cells were stably transduced with a doxycycline-inducible shRNA targeting ATF4. Cells were treated with 1  $\mu$ g/mL doxycycline for 48 hours and MP-A08 (20  $\mu$ M) for 6 hours before cell lysis for immunoblot analysis. ns, a nonspecific band. (G) Chromatin immunoprecipitation analysis of the Noxa promoter in response to MP-A08 treatment (20  $\mu$ M) of MV411 cells for 6 hours. Statistical significance was assessed by Student *t* test. \**P* < .05 (*n* = 4). (H) Primary AML samples were treated with increasing concentrations of MP-A08 and subjected to immunoblot analysis with the indicated antibodies. All qualitative data are representative of at least 3 independent experiments, and all quantitative data represent the mean  $\pm$  standard error of the mean of at least 3 independent experiments.

### SPHK1 inhibition induces ATF4-dependent Noxa transcription

Tumor suppressor TP53 has been shown to directly induce Noxa transcription in response to chemotherapeutics.<sup>18</sup> Unlike daunorubicin and cytarabine, MP-A08 treatment of multiple AML cell lines was associated with a lack of increased TP53 expression, suggesting that the increase in Noxa is independent of TP53 (Figure 2A; supplemental Figure 4). Previous work investigating the mechanism of MP-A08-induced AML cell death, using Ingenuity Pathways Analysis of RNA-sequencing (RNA-seq) data, revealed enrichment of genes associated with the unfolded protein response (UPR).<sup>12</sup> In response to cellular

stresses that cause misfolded proteins to accumulate within the endoplasmic reticulum (ER), cells activate the 3 UPR transmembrane proteins ATF6 (activating transcription factor-6), IRE1 (inositol-requiring kinase 1), and protein kinase R-like ER kinase (PERK) to reestablish proteostasis (Figure 2B). Further examination of this RNA-seq data revealed that MP-A08 treatment of MV411 cells induced almost exclusively activation of the PERK arm of the UPR, typified by upregulation of ATF4 and downstream effectors, including CHOP (supplemental Figure 5A).<sup>12</sup> Direct protein analysis of this pathway demonstrated that MP-A08 induced clear activation/phosphorylation of eIF2a, a central component of the pathway, and induction of ATF4 in

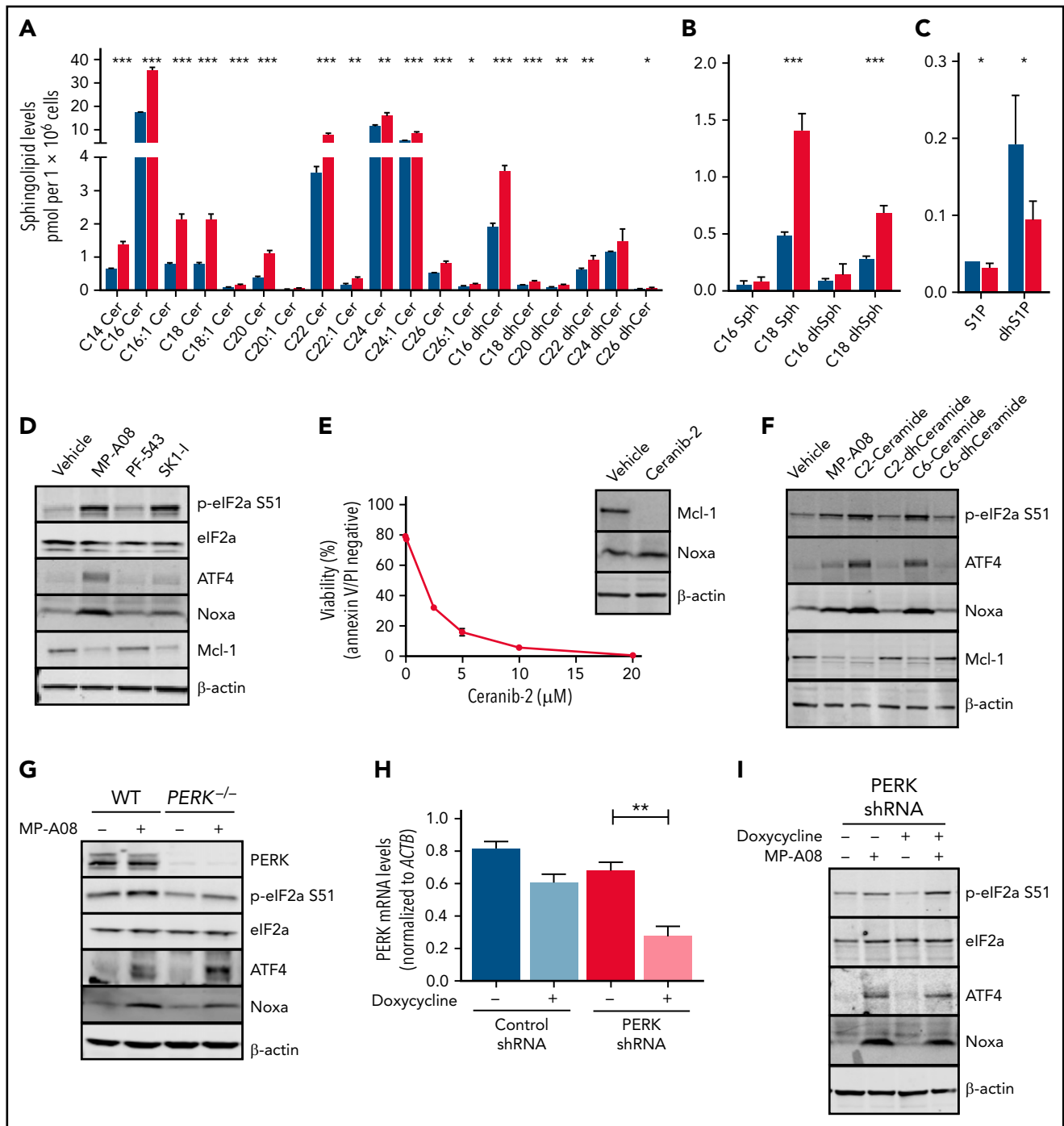


**Figure 3. Ceramides drive a PERK-independent ISR.** (A-C) MV411 cells were treated with vehicle control (0.1% dimethyl sulfoxide [DMSO]; blue bars) or 20 μM MP-A08 (red bars) for 6 hours and analyzed by liquid chromatography-mass spectrometry. (A) Quantitation of individual ceramide (Cer) and dihydroceramide (dhCer) species. (B) Quantitation of sphingosine (Sph) and dihydrosphingosine (dhSph) species. (C) Quantitation of S1P and dihydrosphingosine 1-phosphate (dhS1P). All data are presented as picomoles per million cells; mean ± standard deviation of 4 independent experiments. Statistical significance was assessed by Student t test. \* $P < .05$ ; \*\* $P < .01$ ; \*\*\* $P < .001$ . (D) MV411 cells were treated with MP-A08 (20 μM), PF-543 (1 μM), and SK1-1 (10 μM) for 6 hours; lysed; and subjected to immunoblot analysis. (E) MV411 cells were treated with ceranib-2 for 16 hours and assessed for cell viability by Annexin V/propidium iodide staining. Data are the mean ± standard deviation of 2 independent experiments. MV411 cells were treated with ceranib-2 (10 μM) for 6 hours and subjected to immunoblot analysis with the indicated antibodies. (F) MV411 cells were treated with MP-A08 (20 μM), C2-ceramide (10 μM), C6-ceramide (10 μM), C2-dhCeramide (10 μM), and C6-dhCeramide (10 μM) (all introduced from 2.5 mM stock solutions in dimethyl sulfoxide) for 6 hours; lysed; and subjected to immunoblot analysis with the indicated antibodies. (G) HAP1 wild-type and  $PERK^{-/-}$  cells were treated with MP-A08 (20 μM) for 6 hours, lysed, and subjected to immunoblot analysis with the indicated antibodies. (H-I) MV411 cells were stably transduced with a doxycycline-inducible shRNA targeting PERK. Cells were treated with 1 μg/mL doxycycline for 48 hours and MP-A08 (20 μM) for 6 hours before (H) quantitative PCR analysis of PERK messenger RNA levels and (I) immunoblot analysis with the indicated antibodies. Data are the mean ± standard error of the mean of 3 independent experiments. Statistical significance was assessed by Student t test. \*\* $P < .01$ .

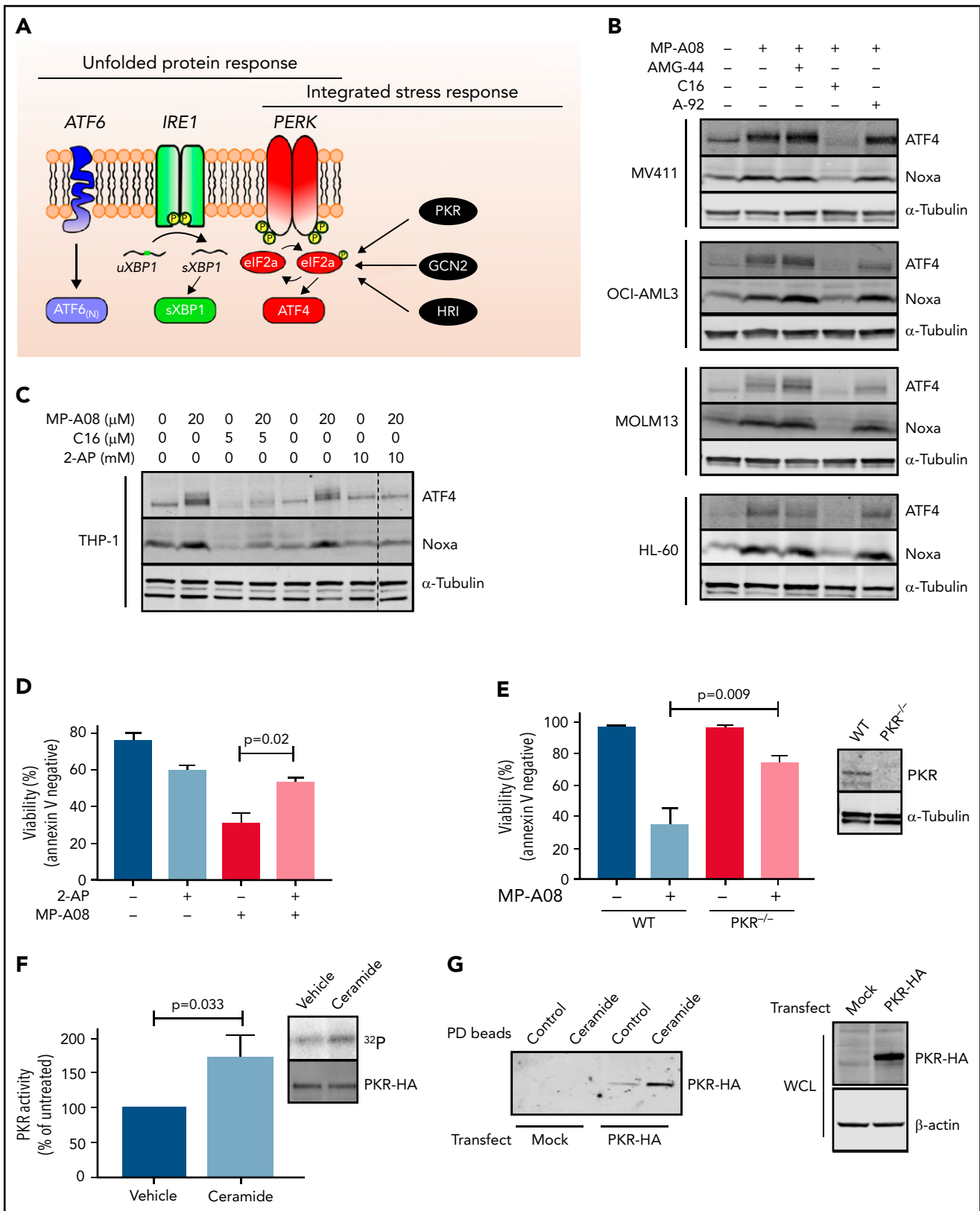


**Figure 4. Ceramides drive a PKR-dependent integrated stress response.** (A) The ISR. (B-C) MV411, OCI-AML3, MOLM13, HL-60, and THP-1 cells were treated with MP-A08 alone (20  $\mu\text{M}$ ) or in combination with the GCN2 inhibitor A-92 (5  $\mu\text{M}$ ), PKR inhibitors C16 (5  $\mu\text{M}$ ) or 2-AP (0.1-10 mM) or PERK inhibitor AMG-44 (5  $\mu\text{M}$ ) for 6 hours before immunoblot analysis with the indicated antibodies. (D) MV411 cells were treated with MP-A08 (10  $\mu\text{M}$ ) and 2-AP (5 mM) for 16 hours and assessed for cell viability by Annexin V/propidium iodide staining. Data are the mean  $\pm$  standard error of the mean (SEM) of 3 independent experiments. Statistical significance was assessed by Student t test. (E) Wild-type (WT) or PKR knockout MV411 cells were treated with MP-A08 (15  $\mu\text{M}$ ) for 16 hours and assessed for cell viability by Annexin V/propidium iodide staining. Data are the mean  $\pm$  SEM of 4 independent experiments. Statistical significance was assessed by Student t test. Immunoblot analysis of

AML cell lines (Figure 2C; supplemental Figure 5B). Similar effects were also observed with CRISPR/Cas9-mediated knock-out of SPHK1 (Figure 2D; supplemental Figure 5C). Intriguingly, consistent with the RNA-seq data, no changes in XBP1 splicing were observed in response to MP-A08 treatment (supplemental Figure 5D), further demonstrating that the effects induced by SPHK1 inhibition are limited to the PERK arm of the UPR. Notably, prolonged activation of the PERK pathway can culminate in upregulation of the BH3-only proteins Noxa and Bim through the transcription factors ATF4 and CHOP, respectively.<sup>19,20</sup> To confirm that ATF4 is necessary to mediate Noxa transcription in response to MP-A08, we used the eIF2b agonist ISRIB to render cells insensitive to eIF2a phosphorylation and block ATF4 production,<sup>21</sup> which nullified the Noxa transcription observed with MP-A08 treatment (Figure 2E; supplemental Figure 1). An ATF4 shRNA recapitulated the effects of ISRIB (Figure 2F; supplemental Figure 6). Chromatin immunoprecipitation analysis of the Noxa promoter confirmed the involvement of ATF4 in Noxa transcription with significant enrichment of ATF4 after MP-A08 treatment (Figure 2G). As observed in the AML cell lines, MP-A08 treatment resulted in dose-dependent increases in eIF2a phosphorylation, Noxa expression, and ATF4 expression in a series of primary AML blasts from patients (Figure 2H).

### Ceramide accumulation activates an apoptotic ISR

Ceramides have been shown to evoke UPR activation and contribute to disease pathogenesis.<sup>22</sup> Furthermore, saturated lipids, of which the ceramides and other sphingolipids are a major class, have been shown to induce IRE1 and PERK activation independent of unfolded proteins via direct sensing of the lipid composition within the ER membrane.<sup>23-26</sup> As the ER is the main location of de novo sphingolipid biosynthesis, we hypothesized that the accumulation of sphingolipids, such as ceramides, at this site in response to SPHK1 inhibition may facilitate the PERK activation observed in response to MP-A08. Indeed, mass spectrometric lipidomic analysis of MV411 cells treated with MP-A08 for 6 hours revealed a broad increase in the cellular levels of various ceramides and dihydroceramides, as well as sphingosine and dihydrosphingosine (Figure 3A-C). Similar MP-A08-induced increases in ceramides, but not in dihydroceramides, were observed in MOLM13 and OCI-AML3 cells, with an apparent bias toward increases in long-chain ceramides over very-long-chain ceramides (supplemental Figure 7). In MV411 cells, increases in ceramides and dihydroceramides were observed as early as 2 hours (supplemental Figure 8), in alignment with the upregulation of ATF4 and Noxa observed at this time point after SPHK1 inhibition by MP-A08 (Figure 2C). Consistent with a role for ceramides/dihydroceramides in these effects, use of PF-543, a potent SPHK1 inhibitor that blocks S1P generation, but inexplicably does not increase ceramide levels,<sup>27</sup> did not induce eIF2a phosphorylation, increase ATF4 and Noxa levels, or reduce Mcl-1 levels (Figure 3D). In contrast, the ceramidase inhibitor ceranib-2, known to elevate cellular ceramide levels,<sup>28</sup> caused induction of Noxa and loss of Mcl-1, as well as the effective cell death of AML cell lines (Figure 3E; supplemental Figure 9). Together, the data suggest that accumulation of ceramides

mediates the anti-AML effects of SPHK1 inhibition, rather than loss of S1P signaling. Indeed, addition of exogenous S1P failed to rescue AML cell death induced by MP-A08 (supplemental Figure 10). To more directly examine the effects of ceramide, we added exogenous C2- or C6-ceramide to MV411 cells, and, unlike the respective dihydroceramides, it induced ATF4 and Noxa expression and loss of Mcl-1, consistent with a role for ceramides in evoking activation of the ATF4 pathway (Figure 3F).

Because our data demonstrated a clear involvement of eIF2a and ATF4 in mediating the effects of SPHK1 inhibition on Noxa accumulation, we next examined the dependency on PERK through the use of both CRISPR/Cas9 knockout of PERK in HAP1 chronic myeloid leukemia cells and doxycycline-inducible shRNA knockdown of PERK in MV411 cells. Unexpectedly, loss of PERK had no effect on MP-A08-induced ATF4 and Noxa accumulation (Figure 3G-I), suggesting that this effect may be driven by an alternative mechanism leading to activation/phosphorylation of eIF2a.

### Ceramides drive an ISR via direct activation of PKR

In addition to PERK, eIF2a can be phosphorylated by 3 other protein kinases that are activated under various stress conditions as part of the ISR. These kinases, PKR, GCN2 (general control nonderepressible 2), and HRI (heme-regulated inhibitor), can all phosphorylate eIF2a to increase translation of the master ISR transcription factor ATF4<sup>29</sup> (Figure 4A). Pharmacological interrogation of the role of these kinases in ATF4 and Noxa induction revealed a clear role for PKR with the 2 PKR inhibitors C16<sup>30</sup> and 2-aminopurine (2-AP)<sup>31</sup> both blocking the effects of MP-A08 (Figure 4B-C). In contrast, inhibition of GCN2 (with A-92) or PERK (with AMG-44) had little or no effect (Figure 4B). Similar effects were observed in all 5 AML cell lines examined (Figure 4B-C). Furthermore, the anti-AML effects of MP-A08 on THP-1 and HL-60 cells were mitigated by either pharmacological targeting of PKR with 2-AP (Figure 4D; supplemental Figure 11) or CRISPR/Cas9 knockout of PKR in MV411 cells (Figure 4E). Collectively, these results indicate a critical role for PKR in sensing SPHK1-inhibitor-induced ceramide accumulation, culminating in activation of eIF2a, leading to activation of ATF4 and Noxa, loss of Mcl-1, and consequent AML cell death.

Previous findings that ceramide can directly modulate the function of various proteins,<sup>32-37</sup> suggest the potential for PKR to be directly activated by ceramide. To investigate, we assessed the effect of ceramide on the activity of isolated PKR *in vitro*. Strikingly, our results demonstrated enhanced PKR activity in the presence of ceramide, suggesting that ceramide directly binds and enhances PKR kinase activity (Figure 4F). To further assess the interaction of ceramide with PKR, we used ceramide-conjugated agarose beads to probe cell lysates for PKR. The data (Figure 4G) demonstrate a clear pull-down of PKR with ceramide beads, compared with control beads, indicative of an interaction of PKR with ceramide.

**Figure 4 (continued)** WT or PKR knockout MV411 cells with the indicated antibodies. (F) PKR-HA was immunoprecipitated from transiently transfected HEK 293T cells, incubated with exogenous C6-ceramide (10  $\mu$ M) for 30 minutes and subjected to a PKR activity assay, using autophosphorylation as the readout. Data are the mean  $\pm$  SEM of 4 independent experiments. (G) Lysates from HEK293T cells transfected with pcDNA3/PKR-HA was incubated with ceramide conjugated to agarose beads or control beads overnight at 4°C, washed, and resolved by sodium dodecyl sulfate-polyacrylamide gel electrophoresis, and the associated PKR was detected by immunoblot analysis with anti-HA antibodies on an Odyssey imaging system.

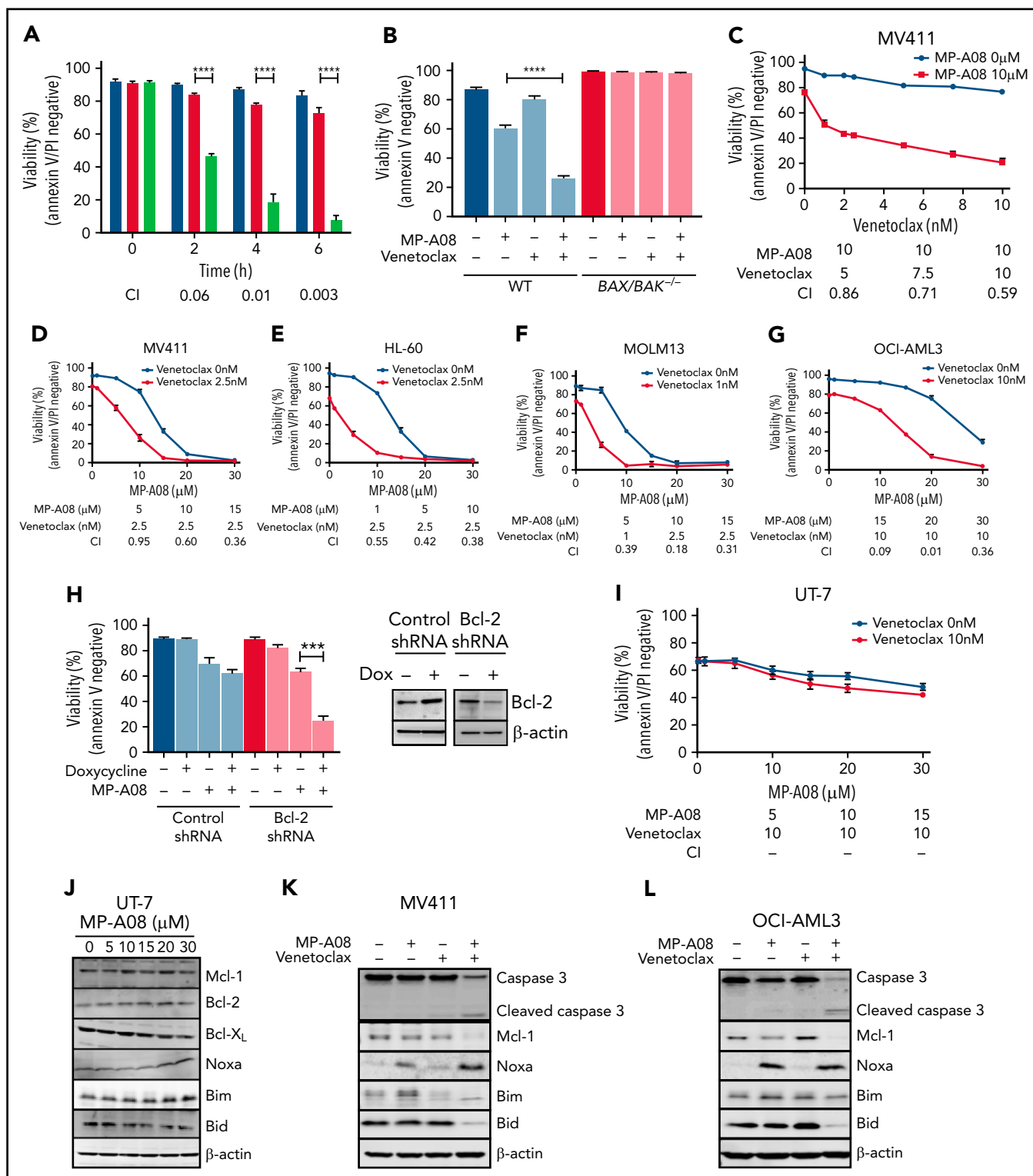


**Figure 5. MP-A08 and venetoclax induces potent synergistic activity in AML cell lines.** (A) MV411 cells were treated for up to 6 hours with 20  $\mu$ M MP-A08 (blue bars), 10 nM venetoclax (red bars), alone or in combination (green bars). Cell viability was analyzed every 2 hours by Annexin V/propidium iodide staining. Data are means  $\pm$  standard error of the mean (SEM; n = 4). Statistical significance was assessed by Student t test. \*\*\*\*P < .0001. Drug synergy was assessed by the Chou-Talay combination index (CI) method whereby CI values <1 are classified as synergy. (B) Factor-dependent myeloid wild-type and Bax/Bak<sup>-/-</sup> cells treated with MP-A08 (20  $\mu$ M) and/or venetoclax (10 nM). Data are the mean  $\pm$  SEM (n = 4). Statistical significance was assessed by Student t test. \*\*\*\*P < .0001. MV411 (C-D), HL-60 (E), MOLM13 (F), and OCI-AML3 (G). (H) MV411 cells were stably transduced with a doxycycline-inducible shRNA targeting Bcl-2 and treated with doxycycline (1  $\mu$ g/mL) for 48 hours and MP-A08 (10  $\mu$ M) for 24 hours. Cell viability was assessed by Annexin V staining. All data are the mean  $\pm$  SEM of 3 independent experiments. Statistical significance was assessed by Student t test. \*\*\*\*P < .0001. (I) UT-7 cells were treated with MP-A08 and venetoclax for 24 hours and assessed for cell viability by Annexin V/propidium iodide staining. Drug synergy was assessed using the Chou-Talay CI method. (J) UT-7 cells were treated with increasing concentrations of MP-A08 for 6 hours and subjected to immunoblot analysis. MV411 (K) and OCI-AML3 (L) cells were treated with MP-A08, venetoclax, or in combination for 6 hours and subjected to immunoblot analysis with the indicated antibodies. All qualitative data are representative of at least 3 independent experiments, and all quantitative data are the mean  $\pm$  SEM of at least 3 independent experiments.



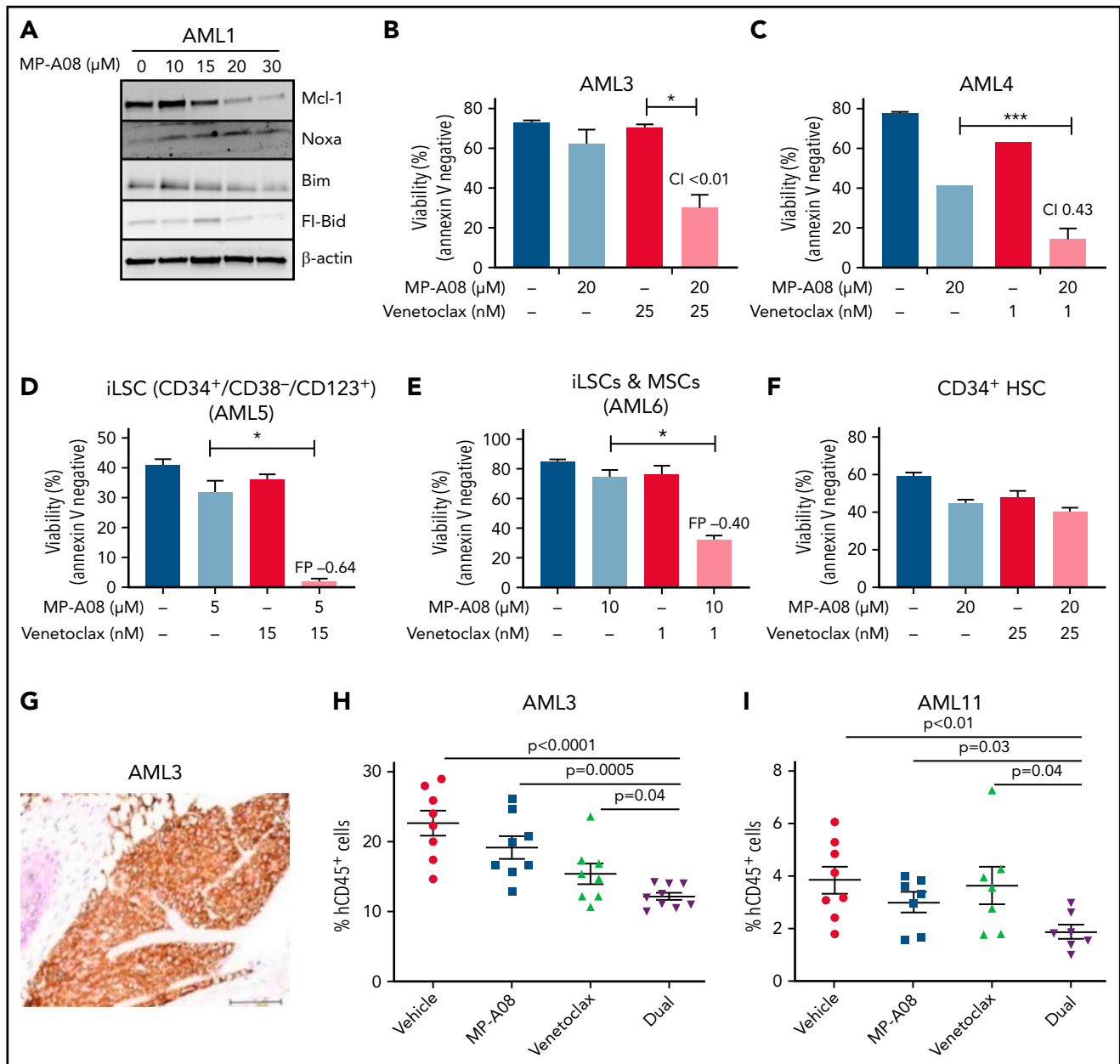


**Figure 6. MP-A08 and venetoclax treatment exhibits antileukemic activity in primary AML samples.** (A) Primary AML cells were treated with increasing concentrations of MP-A08 for 6 hours, lysed, and subjected to immunoblot analysis with indicated antibodies. (B-C) Primary AML samples were treated with MP-A08 and venetoclax for 6 hours and assessed for cell viability by Annexin V staining. Data are displayed as the mean  $\pm$  range of duplicate technical replicates. Statistical significance was assessed by Student *t* test. \**P* < .05; \*\*\**P* < .0005. Synergy was determined by the CI method. Fluorescence-activated cell sorting-purified iLSCs were seeded alone (D) or on an MSC coculture layer (E), treated with MP-A08 and venetoclax for 24 hours, and assessed for cell viability by Annexin V staining. Data are displayed as the mean  $\pm$  range of duplicate technical replicates. Statistical significance was assessed by Student *t* test. \**P* < .05. Synergy was determined by the Webb fractional product method. (F) Normal bone marrow-derived CD34<sup>+</sup> cells were treated with MP-A08 and venetoclax for 24 hours and assessed for cell viability by Annexin V staining. Data are displayed as the mean  $\pm$  range of duplicate technical replicates. (G) Representative immunohistochemistry staining using human specific mitochondrial antibody (MTC02) of an NSG mouse sternum engrafted with primary AML cells. Bar represents 100  $\mu$ m. (H-I) NSG mice were engrafted with primary AML blasts and bled weekly to confirm disease engraftment (>1% hCD45<sup>+</sup> in peripheral blood). Mice received vehicle, MP-A08 (100 mg/kg intraperitoneally), venetoclax (75 mg/kg orally), or both daily for 2 weeks. Engraftment was quantified by assessing the percentage of human CD45<sup>+</sup> cells in the bone marrow of recipient mice. Each symbol represents the percentage of CD45<sup>+</sup> cells observed in a separate mouse. Significance was assessed by Student *t* test. (J) Mutational analysis of AML patient samples treated with venetoclax from the Beat AML Project.<sup>46</sup> The average area under the curve (AUC) is a measure of drug sensitivity (the higher the AUC, the more resistant) derived from ex vivo drug sensitivity assays. Statistical significance was assessed by Student *t* test with Welch's correction. \*\**P* < .01; \*\*\**P* < .0001. (K) Primary AML samples identified by whole-exome sequencing containing PTPN11, TP53 (L), or K-Ras (M) mutations were treated with MP-A08 and venetoclax for 6 hours and assessed for cell viability by Annexin V staining. Data are displayed as the mean  $\pm$  range of duplicate technical replicates. Statistical significance was assessed by Student *t* test. \*\**P* < .01.

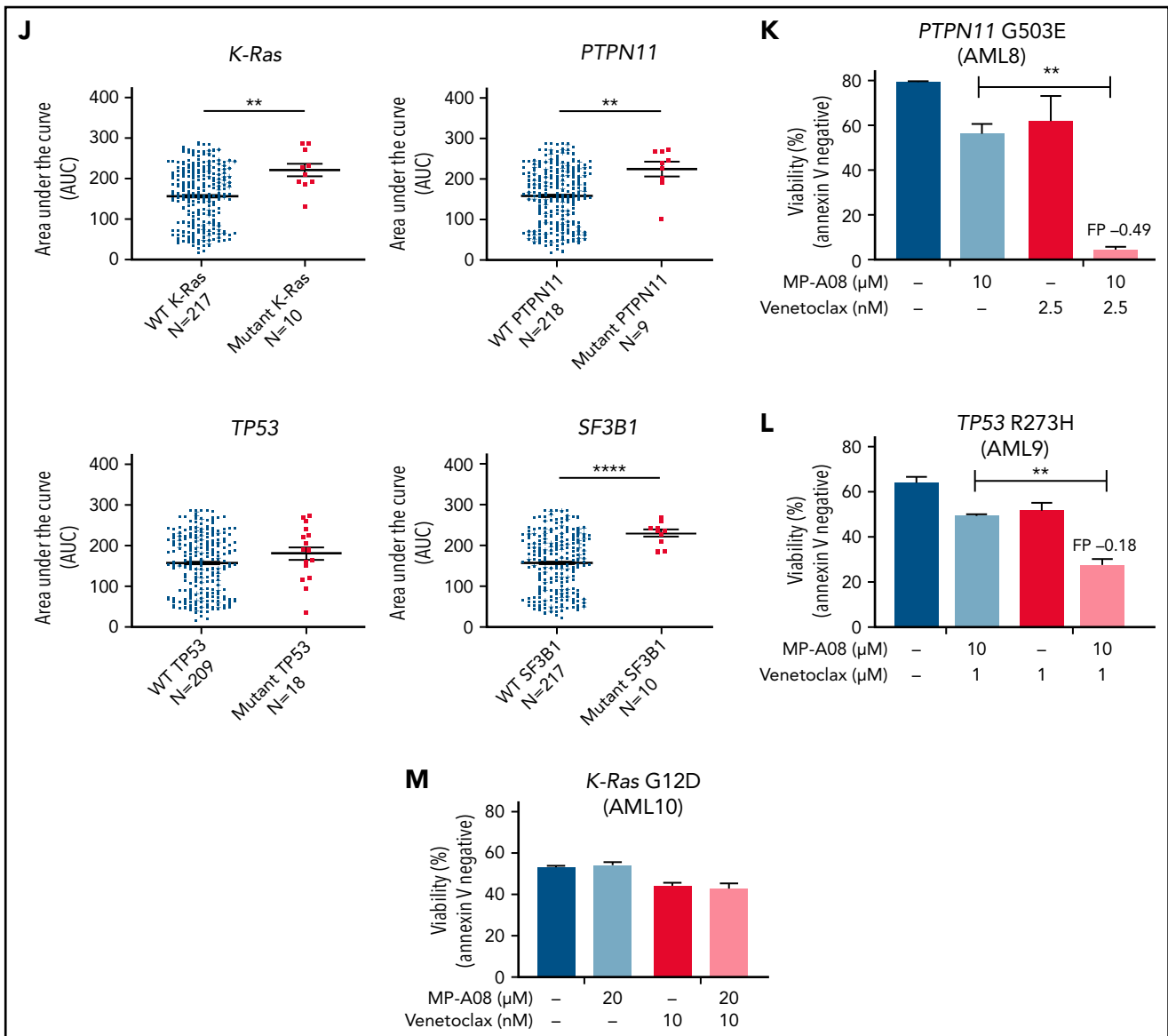


Figure 6. (continued)

### SPHK1 inhibition synergizes with venetoclax in AML cell lines

Mcl-1 is known to mediate resistance to Bcl-2 inhibition in AML,<sup>8</sup> and approaches to target Mcl-1 have been shown to enhance the efficacy of Bcl-2 inhibition in inducing AML cell death.<sup>12,38-42</sup> Thus, we next investigated the therapeutic potential for modulating sphingolipid signaling to affect Bcl-2 antagonism. Anti-AML synergy of MP-A08 and venetoclax was observed as early as 2 hours (Figure 5A) and coupled with enhanced association of Noxa with Mcl-1 (supplemental Figure 12A-B).

Viability studies on factor-dependent myeloid cell lines from wild-type and *Bax*<sup>-/-</sup>/*Bak*<sup>-/-</sup> mice<sup>43</sup> demonstrated that wild-type cells underwent synergistic cell death in response to MP-A08 and venetoclax, but *Bax*<sup>-/-</sup>/*Bak*<sup>-/-</sup> cells were completely resistant (Figure 5B), verifying mitochondria-mediated apoptosis via the executioner proteins Bax and Bak.

Combining MP-A08 with subcytotoxic doses of venetoclax strongly enhanced cell death in venetoclax-sensitive MV411, HL-60, and MOLM13 cell lines (Figure 5C-F), as well as in the venetoclax-resistant OCI-AML3 cell line (Figure 5G). Statistical analysis using the Chou-Talalay method<sup>44</sup> confirmed that combinational treatment induced synergistic cell death (synergy = combination index <1). Treatment of MV411 cells with another SPHK1 inhibitor, SK1-I, recapitulated the effects observed with MP-A08, causing synergistic loss of cell viability with venetoclax treatment (supplemental Figure 12C). Synergy between SPHK1 and Bcl-2 inhibition was further confirmed by doxycycline-inducible shRNA targeting of Bcl-2 in MV411 cells (Figure 5H). Interestingly, at doses capable of achieving drug synergy in other cells, MP-A08 and venetoclax treatment exhibited little effect in UT7 cells (Figure 5I). This lack of response to either drug, however, may be explained either by the strong expression of Bcl-X<sub>L</sub> (supplemental Figure 12D)<sup>45</sup> or by the lack of

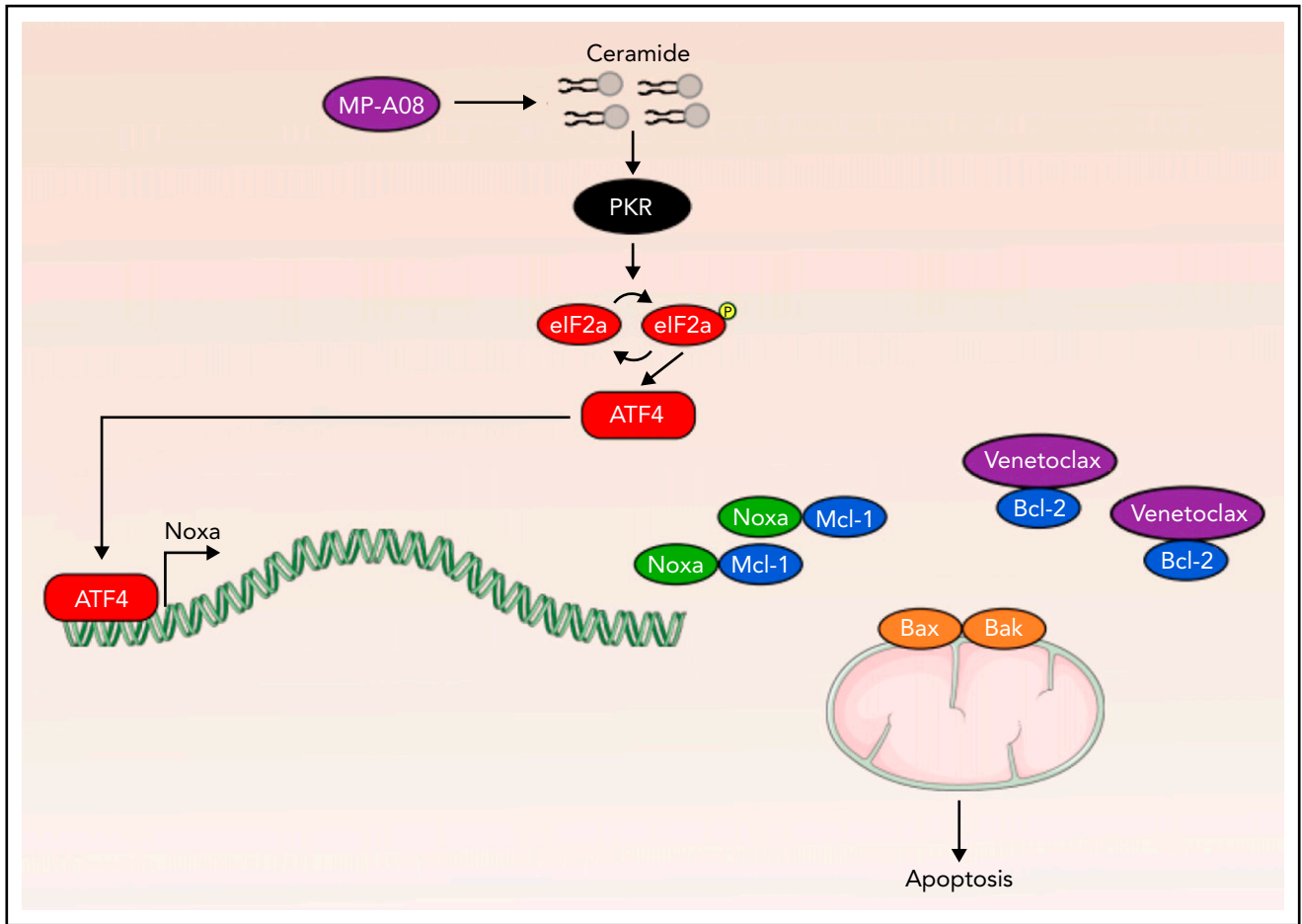


**Figure 7. Ceramides induce ISR activation and sensitize cells to Bcl-2 inhibition.** The accumulation of proapoptotic sphingolipids, such as ceramide, in response to SPHK inhibition is sensed by the eIF2a kinase PKR. PKR activation culminates in an apoptotic ISR mediated by master transcription factor ATF4. ATF4 promotes Bcl-2 dependency by the transcriptional upregulation of Noxa and the subsequent binding to and inactivation of Mcl-1.

Mcl-1 degradation in response to MP-A08 (Figure 5J). Combined treatment was associated with synergistic activation of caspase 3 and loss of Mcl-1 across several AML cell lines (Figure 5K-L; supplemental Figure 12E).

### MP-A08 and venetoclax treatment exhibits antileukemic activity in primary AML cells in vitro and in vivo

MP-A08 treatment of primary AML samples induced changes in levels of Mcl-1, Noxa, and Bid (Figure 6A). Combining MP-A08 and venetoclax also resulted in synergistically enhanced cell death of primary AML blasts from patients (Figure 6B-C) and chemorefractory and relapse-driving iLSCs (Figure 6D) even when cocultured with human bone marrow–derived mesenchymal stem cells (Figure 6E; supplemental Figure 13A). This result suggests that a dual-targeting approach is sufficient to induce cell death across different AML subtypes, even in the presence of extrinsic factor support from mesenchymal stem cells. Further analysis also showed that combining MP-A08 and venetoclax reduced colony-forming units in human primary AML cells (supplemental Figure 13B). Notably, however, even high concentrations of MP-A08 and venetoclax had minimal effects on CD34<sup>+</sup> hematopoietic stem/progenitor cells isolated from healthy volunteers (Figure 6F; supplemental Figure 13C).

We next assessed the efficacy of MP-A08 and venetoclax in vivo using human primary AML xenografts in NSG mice. Immunohistochemical staining for human leukemic cells in the sternum confirmed systemic orthotopic engraftment in 2 separate sets of primary AML xenografts from patients (Figure 6G). Mice with established disease were treated daily with MP-A08 (100 mg/kg), venetoclax (75 mg/kg), or the combination for 2 weeks. This combinational approach significantly reduced the leukemic engraftment compared with the respective monotherapies, as assessed by flow cytometric analysis of hCD45<sup>+</sup> cells in the bone marrow of these mice (Figure 6H-I). Notably, similar dual therapy with MP-A08 and venetoclax daily for 2 weeks in control C57Bl/6 mice showed no obvious toxicity, with no deleterious effects on body weight, major bone marrow lineages, or blood cell counts (supplemental Figure 14).

Because MP-A08 enhanced venetoclax-induced killing of AML cells, we sought to expand this finding by identifying venetoclax-resistant patients using the Beat AML Master Trial data (ex vivo drug sensitivity analysis with 122 drugs on 409 patient samples) to assess whether these patients could be resensitized to venetoclax.<sup>46</sup> In addition to the TP53<sup>mut</sup> cohort identified in the phase 2 studies of venetoclax with cytarabine or hypomethylating agents,<sup>6,47</sup> we identified patients with KRAS, PTPN11, and SF3B1 mutations as resistant to venetoclax

treatment (Figure 6J), consistent with previous findings.<sup>40</sup> Combined MP-A08 and venetoclax treatment exhibited synergistic anti-AML activity in diagnostic patient samples containing either *PTPN11* or *TP53* mutations (supplemental Table 1; Figure 6K-L) with little effect in patient cells containing a *KRAS* mutation (Figure 6M). Although only from single patients with each mutation, collectively, the data begin to provide preclinical evidence for combination therapy with SPHK1 inhibitors to augment the efficacy of venetoclax in a variety of AML subtypes.

## Discussion

The success of the Bcl-2 inhibitor venetoclax in chronic lymphocytic leukemia has revolutionized the therapeutic landscape. Yet, in AML, which relies on Mcl-1 for survival,<sup>7</sup> the modest single-agent activity of venetoclax has fueled the search for new therapies that can be combined with this drug.<sup>4</sup> In this study, we found that enhancing ceramide accumulation through targeting SPHK1 may be such an approach, with ceramide directly activating PKR; inducing ATF4-mediated transcriptional upregulation of Noxa, a known inducer of Mcl-1 degradation; and acting synergistically with venetoclax to induce apoptosis in AML cells. This synergy extended to both primary AML blasts and iLSCs, suggesting this combinational approach may reduce relapse rates by depleting leukemia-initiating cells. Importantly, this approach also reduced disease engraftment in orthotopic models involving xenografts from patients with AML, providing preclinical evidence of the targeting of SPHK1 and Bcl-2 as a valid combinational approach in treating AML.

The Beat AML Master Trial is a multicenter clinical trial integrating genomics data with in vitro responses to both clinical and preclinical agents.<sup>46</sup> Using these data, we identified patients with several mutations, including those in *KRAS*, *PTPN11*, and *SF3B1*, to confer venetoclax resistance in addition to the TP53<sup>Mut</sup> cohort observed in a phase 2 study examining cytarabine and venetoclax.<sup>6</sup> In an exciting finding, SPHK1 inhibition combined with venetoclax was effective in patient samples containing *PTPN11* or *TP53* mutations (Figure 5J-K). The absence of any effect observed in a *KRAS*-mutated case may be related to the protective effects of *KRAS* in activating the IRE1 pathway to promote survival, as observed in HSCs.<sup>48</sup> Follow-up analysis with cells from further patients with *KRAS*-mutated AML is clearly necessary to confirm whether these apparent protective effects of mutant *KRAS* against venetoclax/SPHK1 inhibition holds true. Notably, our analysis suggests AML with *NRAS* mutations, which are more common,<sup>49</sup> remain sensitive to combination therapy with venetoclax/SPHK1 inhibition, as demonstrated by data from HL-60 and OCI-AML3 cell lines (Figure 5E,G) and patient sample AML11 (Figure 6I). Collectively, this result suggests that SPHK1 inhibition may be an effective therapy in combination with venetoclax in patients who are venetoclax insensitive. Because SPHK1 inhibition increases Noxa in a manner independent of TP53, its combination with drugs such as cytarabine that are ineffective in cohorts such as patients with a TP53 mutation, may also be warranted.

Approaches to enhance cellular ceramide as a potential anti-AML therapy have been investigated over the past 2 decades,<sup>10</sup> including those with inhibitors of SPHK1<sup>12,13,50</sup> and acid ceramidase<sup>51,52</sup> and more recently with direct nanoliposomal ceramide formulations.<sup>53,54</sup> The mechanisms whereby ceramide elicits its

anti-AML effects, however, have not been clear. In this study, we showed that accumulation of ceramides through SPHK1 inhibition activates an apoptotic ISR that is dependent on PKR. Although ISR activation has been reported previously in response to addition of exogenous ceramides,<sup>55</sup> this is the first time to our knowledge that endogenous ceramides have been associated with ISR activation, and it is the first report of direct activation of PKR by ceramides. Furthermore, we have provided evidence that Noxa is a significant effector of the apoptotic effects of ceramide accumulation through the ISR, expanding the role of sphingolipids in dictating cell survival, thus building on previous studies suggesting that ceramide acts both before apoptosis, through Bcl-2 dephosphorylation<sup>56</sup> and Bad activation,<sup>57</sup> and during apoptosis through the formation of ceramide-induced channels in the mitochondrial outer membrane, to facilitate release of cytochrome c and other proapoptotic mediators.<sup>58</sup>

Notably, an oncogenic role for PKR in AML has been reported, with high PKR expression in AML associated with poor patient prognosis, apparently because of the suppressive effects of PKR on the DNA damage response, an important feature of efficacy to chemotherapeutics, such as cytarabine and daunorubicin.<sup>59</sup> Thus, these observations, combined with the findings of the current study that show that the anti-AML effects of SPHK1 inhibition appear to be independent of TP53 and DNA damage response activation and dependent on PKR activation, make it tempting to speculate that high PKR-expressing patients may respond better to SPHK1 inhibition than to chemotherapy.

Our findings support a prominent role for the PKR/ATF4/Noxa/Mcl-1 axis identified in this study in mediating ceramide-induced AML cell death. However, efficient Noxa knockdown does not completely rescue AML cell killing by MP-A08 (Figure 1F), supporting the notion that other pathways may play minor roles in the anti-AML effects of MP-A08. Our analysis of gene expression changes in AML cells in response to MP-A08<sup>12</sup> suggest a range of altered pathways that may be involved, including oxidative stress and autophagy, as well as other target genes downstream of ATF4 and one of its effectors, CHOP (supplemental Table 2). This possibility warrants further investigation.

Recent work has revealed the important role of ATF4, the master regulator of the ISR, in survival of leukemia.<sup>60,61</sup> In particular, ATF4 has been shown to promote cell survival in FLT3-ITD<sup>+</sup> AML by enhancing autophagy.<sup>62</sup> Others have shown that primitive LSCs exhibit higher basal ISR activity and ATF4 levels than leukemic progenitors/blasts, which may protect LSCs against amino acid deprivation.<sup>60</sup> Yet, we and others have found that ATF4 can prime cancer cells for apoptosis via transcriptional upregulation of Noxa.<sup>20,63</sup> Determining how LSCs control the dichotomous signaling of ATF4 to favor survival signaling and how ceramide disrupts this process requires further investigation. As ATF4 is regulated by phosphorylation,<sup>64</sup> we cannot discount the premise that ceramide, a known activator of protein phosphatases, including PP2A,<sup>65</sup> may also modulate ATF4 at the posttranslational level. Indeed, a recent study demonstrated that PP2A activation causes upregulation of ATF4 and Noxa, strengthening the potential link between ceramide and the ISR.<sup>66</sup> Furthermore, ceramides induces loss of oxidative phosphorylation, a metabolic vulnerability of quiescent LSPCs.<sup>67,68</sup> Collectively, these findings suggests that ceramide-inducing

agents, together with venetoclax, may represent an LSC-specific therapy by activating the ISR, reducing the likelihood of relapse and chemotherapy-resistant disease (Figure 7).

## Acknowledgments

The authors thank the South Australian Cancer Research Biobank (SACRB) and the patients who donated samples and Sarah Tamang, who provided technical assistance.

This work was supported by a Research Training Program Scholarship and Royal Adelaide Hospital Dawes Top-up scholarship (A.C.L.); the Fay Fuller Foundation, the Royal Adelaide Hospital Research Fund, The Hospital Research Foundation, Senior Research Fellowship GNT1156693 (S.M.P.); Early Career Fellowship PG101400 (T.M.N.); and project grants NT1145139 and GNT1184485 from the National Health and Medical Research Council of Australia. D.T. is supported by the Leukemia and Lymphoma Translation Research Program and a CSL Centenary Fellowship.

## Authorship

Contribution: A.C.L., M.N.T., V.S.P., M.L., G.O.N., T.M.N., C.T.W.-B., P.A.B.M., D.A., D.J.C., M.C., S.R.A., C.A.L.T.-P., B.K.D., A.G.B., M.R.P., B.L.G., and J.A.P. performed the experiments; P.G.E., G.J.G., and N.R. provided intellectual input and/or the reagents; D.M.R., A.L.B., and R.D. provided patient tissue samples and clinical notes; A.C.L., J.A.P., D.T., and S.M.P. designed the studies and analyzed the data; A.C.L., J.A.P., and S.M.P. wrote the manuscript; and all authors critically reviewed and edited the manuscript.

Conflict-of-interest disclosure: The authors declare no competing financial interests.

The current affiliation for A.C.L. is The Peter MacCallum Cancer Centre, Melbourne, VIC, Australia.

ORCID profiles: M.N.T., 0000-0001-7045-1198; C.T.W.-B., 0000-0002-7457-5937; D.A., 0000-0003-0284-471X; D.J.C., 0000-0001-7497-7082; M.C., 0000-0002-2162-6497; C.A.L.T.-P., 0000-0001-7172-3183; B.K.D., 0000-0002-6103-5165; A.G.B., 0000-0003-3876-1537; G.J.G., 0000-0003-1294-0692; P.G.E., 0000-0002-2976-8617; A.L.B., 0000-0002-9023-0138; R.D., 0000-0002-4915-4612; N.R., 0000-0002-7361-9491; M.R.P., 0000-0002-9587-3837; D.M.R., 0000-0001-7171-2935; J.A.P., 0000-0001-8493-9178; S.M.P., 0000-0002-9527-2740.

Correspondence: Stuart M. Pitson, University of Adelaide, Bradley Building, North Terrace, Adelaide, SA 5001, Australia; e-mail: stuart.pitson@unisa.edu.au; and Jason A. Powell, University of Adelaide Bradley Building, North Terrace, Adelaide, SA 5001, Australia; e-mail: jason.powell@sa.gov.au.

## Footnotes

Submitted 9 July 2021; accepted 4 April 2022; prepublished online on *Blood* First Edition 20 April 2022. DOI 10.1182/blood.2021013277.

\*J.A.P. and S.M.P. are equal senior authors.

Requests for data sharing may be submitted to Stuart M. Pitson (stuart.pitson@unisa.edu.au).

The online version of this article contains a data supplement.

There is a *Blood* Commentary on this article in this issue.

The publication costs of this article were defrayed in part by page charge payment. Therefore, and solely to indicate this fact, this article is hereby marked "advertisement" in accordance with 18 USC section 1734.

## REFERENCES

1. Albert MC, Brinkmann K, Kashkar H. Noxa and cancer therapy: tuning up the mitochondrial death machinery in response to chemotherapy. *Mol Cell Oncol*. 2014;1(1):e29906.
2. Morsi RZ, Hage-Sleiman R, Kobeissy H, Dbaibo G. Noxa: role in cancer pathogenesis and treatment. *Curr Cancer Drug Targets*. 2018;18(10):914-928.
3. Roberts AW, Davids MS, Pagel JM, et al. Targeting BCL2 with venetoclax in relapsed chronic lymphocytic leukemia. *N Engl J Med*. 2016;374(4):311-322.
4. Konopleva M, Pollyea DA, Potluri J, et al. Efficacy and biological correlates of response in a phase II study of venetoclax monotherapy in patients with acute myelogenous leukemia. *Cancer Discov*. 2016;6(10):1106-1117.
5. Wei AH, Montesinos P, Ivanov V, et al. Venetoclax plus LDAC for newly diagnosed AML ineligible for intensive chemotherapy: a phase 3 randomized placebo-controlled trial. *Blood*. 2020;135(24):2137-2145.
6. DiNardo CD, Tiong IS, Quaglieri A, et al. Molecular patterns of response and treatment failure after frontline venetoclax combinations in older patients with AML. *Blood*. 2020;135(11):791-803.
7. Glaser SP, Lee EF, Trounson E, et al. Anti-apoptotic Mcl-1 is essential for the development and sustained growth of acute myeloid leukemia. *Genes Dev*. 2012;26(2):120-125.
8. van Delft MF, Wei AH, Mason KD, et al. The BH3 mimetic ABT-737 targets selective Bcl-2 proteins and efficiently induces apoptosis via Bak/Bax if Mcl-1 is neutralized. *Cancer Cell*. 2006;10(5):389-399.
9. Newton J, Lima S, Maceyka M, Spiegel S. Revisiting the sphingolipid rheostat: evolving concepts in cancer therapy. *Exp Cell Res*. 2015;333(2):195-200.
10. Lewis AC, Wallington-Beddoe CT, Powell JA, Pitson SM. Targeting sphingolipid metabolism as an approach for combination therapies in haematological malignancies. *Cell Death Discov*. 2018;4(1):72.
11. Pitson SM. Regulation of sphingosine kinase and sphingolipid signaling. *Trends Biochem Sci*. 2011;36(2):97-107.
12. Powell JA, Lewis AC, Zhu W, et al. Targeting sphingosine kinase 1 induces MCL1-dependent cell death in acute myeloid leukemia. *Blood*. 2017;129(6):771-782.
13. Paugh SW, Paugh BS, Rahmani M, et al. A selective sphingosine kinase 1 inhibitor integrates multiple molecular therapeutic targets in human leukemia. *Blood*. 2008;112(4):1382-1391.
14. Dick TE, Hengst JA, Fox TE, et al. The apoptotic mechanism of action of the sphingosine kinase 1 selective inhibitor SKI-178 in human acute myeloid leukemia cell lines. *J Pharmacol Exp Ther*. 2015;352(3):494-508.
15. Hengst JA, Dick TE, Sharma A, et al. SKI-178: a multitargeted inhibitor of sphingosine kinase and microtubule dynamics demonstrating therapeutic efficacy in acute myeloid leukemia models. *Cancer Transl Med*. 2017;3(4):109-121.
16. Hengst JA, Hegde S, Paulson RF, Yun JK. Development of SKI-349, a dual-targeted inhibitor of sphingosine kinase and microtubule polymerization. *Bioorg Med Chem Lett*. 2020;30(20):127453.
17. Czabotar PE, Lee EF, van Delft MF, et al. Structural insights into the degradation of Mcl-1 induced by BH3 domains. *Proc Natl Acad Sci USA*. 2007;104(15):6217-6222.
18. Oda K, Arakawa H, Tanaka T, et al. p53AIP1, a potential mediator of p53-dependent apoptosis, and its regulation by Ser-46-phosphorylated p53. *Cell*. 2000;102(6):849-862.
19. Puthalakath H, O'Reilly LA, Gunn P, et al. ER stress triggers apoptosis by activating BH3-only protein Bim. *Cell*. 2007;129(7):1337-1349.
20. Wang Q, Mora-Jensen H, Weniger MA, et al. ERAD inhibitors integrate ER stress

- with an epigenetic mechanism to activate BH3-only protein NOXA in cancer cells. *Proc Natl Acad Sci USA*. 2009;106(7):2200-2205.
21. Zyryanova AF, Weis F, Failla A, et al. Binding of ISRIB reveals a regulatory site in the nucleotide exchange factor eIF2B. *Science*. 2018;359(6383):1533-1536.
  22. Bennett MK, Wallington-Beddoe CT, Pitson SM. Sphingolipids and the unfolded protein response. *Biochim Biophys Acta Mol Cell Biol Lipids*. 2019;1864(10):1483-1494.
  23. Bennett MK, Li M, Tea MN, et al. Resensitising proteasome inhibitor-resistant myeloma with sphingosine kinase 2 inhibition. *Neoplasia*. 2022;24(1):1-11.
  24. Halbleib K, Pesek K, Covino R, et al. Activation of the unfolded protein response by lipid bilayer stress. *Mol Cell*. 2017;67(4):673-684.e8.
  25. Volmer R, Ron D. Lipid-dependent regulation of the unfolded protein response. *Curr Opin Cell Biol*. 2015;33:67-73.
  26. Volmer R, van der Ploeg K, Ron D. Membrane lipid saturation activates endoplasmic reticulum unfolded protein response transducers through their transmembrane domains. *Proc Natl Acad Sci USA*. 2013;110(12):4628-4633.
  27. Schnute ME, McReynolds MD, Kasten T, et al. Modulation of cellular S1P levels with a novel, potent and specific inhibitor of sphingosine kinase-1. *Biochem J*. 2012;444(1):79-88.
  28. Draper JM, Xia Z, Smith RA, Zhuang Y, Wang W, Smith CD. Discovery and evaluation of inhibitors of human ceramidase. *Mol Cancer Ther*. 2011;10(11):2052-2061.
  29. Pakos-Zebrucka K, Koryga I, Mnich K, Ljubic M, Samali A, Gorman AM. The integrated stress response. *EMBO Rep*. 2016;17(10):1374-1395.
  30. Jammi NV, Whitby LR, Beal PA. Small molecule inhibitors of the RNA-dependent protein kinase. *Biochem Biophys Res Commun*. 2003;308(1):50-57.
  31. Kaufman RJ. Double-stranded RNA-activated protein kinase mediates virus-induced apoptosis: a new role for an old actor. *Proc Natl Acad Sci USA*. 1999;96(21):11693-11695.
  32. Mukhopadhyay A, Saddoughi SA, Song P, et al. Direct interaction between the inhibitor 2 and ceramide via sphingolipid-protein binding is involved in the regulation of protein phosphatase 2A activity and signaling. *FASEB J*. 2009;23(3):751-763.
  33. Heinrich M, Wickel M, Schneider-Brachert W, et al. Cathepsin D targeted by acid sphingomyelinase-derived ceramide. *EMBO J*. 1999;18(19):5252-5263.
  34. Huwiler A, Brunner J, Hummel R, et al. Ceramide-binding and activation defines protein kinase c-Raf as a ceramide-activated protein kinase. *Proc Natl Acad Sci USA*. 1996;93(14):6959-6963.
  35. Zhang Y, Yao B, Delikat S, et al. Kinase suppressor of Ras is ceramide-activated protein kinase. *Cell*. 1997;89(1):63-72.
  36. Dadsena S, Bockelmann S, Mina JGM, et al. Ceramides bind VDAC2 to trigger mitochondrial apoptosis. *Nat Commun*. 2019;10(1):1832.
  37. Fekry B, Jeffries KA, Esmailniakooshkghazi A, et al. C<sub>16</sub>-ceramide is a natural regulatory ligand of p53 in cellular stress response. *Nat Commun*. 2018;9(1):4149.
  38. Ewald L, Dittmann J, Vogler M, Fulda S. Side-by-side comparison of BH3-mimetics identifies MCL-1 as a key therapeutic target in AML. *Cell Death Dis*. 2019;10(12):917.
  39. Niu X, Zhao J, Ma J, et al. Binding of released Bim to Mcl-1 is a mechanism of intrinsic resistance to ABT-199 which can be overcome by combination with daunorubicin or cytarabine in AML cells. *Clin Cancer Res*. 2016;22(17):4440-4451.
  40. Phillips DC, Jin S, Gregory GP, et al. A novel CDK9 inhibitor increases the efficacy of venetoclax (ABT-199) in multiple models of hematologic malignancies. *Leukemia*. 2020;34(6):1646-1657.
  41. Ramsey HE, Fischer MA, Lee T, et al. A novel MCL1 inhibitor combined with venetoclax rescues venetoclax-resistant acute myelogenous leukemia. *Cancer Discov*. 2018;8(12):1566-1581.
  42. Zhang H, Nakauchi Y, Köhne T, et al. Integrated analysis of patient samples identifies biomarkers for venetoclax efficacy and combination strategies in acute myeloid leukemia. *Nat Can*. 2020;1(8):826-839.
  43. Ekert PG, Jabbour AM, Manoharan A, et al. Cell death provoked by loss of interleukin-3 signaling is independent of Bad, Bim, and PI3 kinase, but depends in part on Puma. *Blood*. 2006;108(5):1461-1468.
  44. Chou T-C. Theoretical basis, experimental design, and computerized simulation of synergism and antagonism in drug combination studies. *Pharmacol Rev*. 2006;58(3):621-681.
  45. Soderquist RS, Crawford L, Liu E, et al. Systematic mapping of BCL-2 gene dependencies in cancer reveals molecular determinants of BH3 mimetic sensitivity. *Nat Commun*. 2018;9(1):3513.
  46. Tyner JW, Tognon CE, Bottomly D, et al. Functional genomic landscape of acute myeloid leukaemia. *Nature*. 2018;562(7728):526-531.
  47. Nechiporuk T, Kurtz SE, Nikolova O, et al. The TP53 apoptotic network is a primary mediator of resistance to BCL2 inhibition in AML cells. *Cancer Discov*. 2019;9(7):910-925.
  48. Liu L, Zhao M, Jin X, et al. Adaptive endoplasmic reticulum stress signalling via IRE1 $\alpha$ -XBP1 preserves self-renewal of haematopoietic and pre-leukaemic stem cells. *Nat Cell Biol*. 2019;21(3):328-337.
  49. Yu J, Li Y, Li T, et al. Gene mutational analysis by NGS and its clinical significance in patients with myelodysplastic syndrome and acute myeloid leukemia. *Exp Hematol Oncol*. 2020;9:2.
  50. Bonhoure E, Pchejetski D, Aouali N, et al. Overcoming MDR-associated chemoresistance in HL-60 acute myeloid leukemia cells by targeting sphingosine kinase-1. *Leukemia*. 2006;20(1):95-102.
  51. Tan SF, Liu X, Fox TE, et al. Acid ceramidase is upregulated in AML and represents a novel therapeutic target. *Oncotarget*. 2016;7(50):83208-83222.
  52. Pearson JM, Tan SF, Sharma A, et al. Ceramide analogue SACLAC modulates sphingolipid levels and MCL-1 splicing to induce apoptosis in acute myeloid leukemia. *Mol Cancer Res*. 2020;18(3):352-363.
  53. McGill CM, Brown TJ, Fisher LN, et al. Combinatorial Efficacy of Quercetin and Nanoliposomal Ceramide for Acute Myeloid Leukemia. *Int J Biopharm Sci*. 2018;1(1):106.
  54. Barth BM, Wang W, Toran PT, et al. Sphingolipid metabolism determines the therapeutic efficacy of nanoliposomal ceramide in acute myeloid leukemia. *Blood Adv*. 2019;3(17):2598-2603.
  55. Ruvolo PP, Gao F, Blalock WL, Deng X, May WS. Ceramide regulates protein synthesis by a novel mechanism involving the cellular PKR activator RAX. *J Biol Chem*. 2001;276(15):11754-11758.
  56. Ruvolo PP, Deng X, Ito T, Carr BK, May WS. Ceramide induces Bcl2 dephosphorylation via a mechanism involving mitochondrial PP2A. *J Biol Chem*. 1999;274(29):20296-20300.
  57. Basu S, Bayoumy S, Zhang Y, Lozano J, Kolesnick R. BAD enables ceramide to signal apoptosis via Ras and Raf-1. *J Biol Chem*. 1998;273(46):30419-30426.
  58. Chang KT, Anishkin A, Patwardhan GA, Beverly LJ, Siskind LJ, Colombini M. Ceramide channels: destabilization by Bcl-xL and role in apoptosis. *Biochim Biophys Acta*. 2015;1848(10 Pt A):2374-2384.
  59. Cheng X, Byrne M, Brown KD, et al. PKR inhibits the DNA damage response, and is associated with poor survival in AML and accelerated leukemia in NHD13 mice. *Blood*. 2015;126(13):1585-1594.
  60. van Galen P, Mbong N, Kreso A, et al. Integrated stress response activity marks stem cells in normal hematopoiesis and leukemia. *Cell Rep*. 2018;25(5):1109-1117.e5.
  61. Zhou C, Martinez E, Di Marcantonio D, et al. JUN is a key transcriptional regulator of the unfolded protein response in acute myeloid leukemia. *Leukemia*. 2017;31(5):1196-1205.
  62. Heydt Q, Larrue C, Saland E, et al. Oncogenic FLT3-ITD supports autophagy via

- ATF4 in acute myeloid leukemia. *Oncogene*. 2018;37(6):787-797.
63. Armstrong JL, Flockhart R, Veal GJ, Lovat PE, Redfern CP. Regulation of endoplasmic reticulum stress-induced cell death by ATF4 in neuroectodermal tumor cells. *J Biol Chem*. 2010;285(9):6091-6100.
64. Sharma K, D'Souza RC, Tyanova S, et al. Ultradeep human phosphoproteome reveals a distinct regulatory nature of Tyr and Ser/Thr-based signaling. *Cell Rep*. 2014;8(5):1583-1594.
65. Chalfant CE, Kishikawa K, Mumby MC, Kamibayashi C, Bielawska A, Hannun YA. Long chain ceramides activate protein phosphatase-1 and protein phosphatase-2A. Activation is stereospecific and regulated by phosphatidic acid. *J Biol Chem*. 1999; 274(29):20313-20317.
66. Ryder CB, Narla G. Direct-acting small molecule activators of PP2A (SMAPs) in myeloid malignancies: understanding mechanisms of cytotoxicity to inform rational combinatorial therapeutic strategies [abstract]. *Blood*. 2017; 130(suppl 1):2517.
67. Morad SAF, Ryan TE, Neuffer PD, et al. Ceramide-tamoxifen regimen targets bioenergetic elements in acute myelogenous leukemia. *J Lipid Res*. 2016; 57(7):1231-1242.
68. Lagadinou ED, Sach A, Callahan K, et al. BCL-2 inhibition targets oxidative phosphorylation and selectively eradicates quiescent human leukemia stem cells. *Cell Stem Cell*. 2013;12(3):329-341.

© 2022 by The American Society of Hematology. Licensed under Creative Commons Attribution-NonCommercial-NoDerivatives 4.0 International (CC BY-NC-ND 4.0), permitting only noncommercial, nonderivative use with attribution. All other rights reserved.